Electronic Supplementary Material (ESI) for Nanoscale.

Supporting Information

Tailoring the self-assembly of a tripeptide for the formation of antimicrobial surfaces

Sivan Nir[a], David Zanuy[b], Tal Zada[a], Omer Agazani[a], Carlos Aleman[b], Deborah E. Shalev[c,d]* and Meital Reches[a]**

[a]Institute of Chemistry and The Center for Nanoscience and Nanotechnology, The Hebrew University of Jerusalem, Jerusalem, 91904, Israel.

[b]Department of Chemical Engineering, Universitat Politècnica de Catalunya, ETSEIB, Barcelona, 08028 Spain.

[c]The Wolfson Centre for Applied Structural Biology, The Hebrew University of Jerusalem, Israel

[d]Department of Pharmaceutical Engineering, Azrieli College of Engineering, Jerusalem, Israel

*Corresponding author

Email: *meital.reches@mail.huji.ac.il*

E-mail: david.zanuy@upc.edu

E-mail: debbie@jce.ac.il

Methods

Materials

All chemicals, proteins and bacteria were purchased from commercially available companies and used as supplied unless otherwise stated. The reported peptide was synthesized by a conventional solution-phase method as described before.[1] Doxorubicin, gentamicin, bovine serum albumin BSA, GOx, Atto590-NHS, 2,2'-azino-bis(3-ethylbenzothiazoline-6-sulphonic acid) and Horseradish Peroxidase were obtained from Sigma-Aldrich (Jerusalem, Israel). *Escherichia coli* (ATCC 25922) was purchased from ATCC (Virginia, USA). Luria broth and tryptic soy broth were obtained from BD Difco (New Jersey, USA). Nutrient agar was obtained from Merck (Darmstadt, Germany).

Stock Solution

To avoid any pre-aggregation, a new fresh stock solution was prepared for each experiment. The fresh stock solution was prepared by dissolving the peptide in pure ethanol (Gadot, Israel) to a concentration of 100 mg/mL.

Preparation of Spheres

Peptide Self-Assembly

The peptide stock solution was diluted to a final concentration of 1 mg/mL in either Tris buffer (10 mM, pH=8.5) or 1 M HCl.

High-resolution electron microscopy (HR-SEM)

A 30 µL drop containing the peptide spheres was drop-casted on a glass cover slip and allowed to dry at room temperature (RT). The peptides on the glass were coated with gold using a Polaron SC7640 sputter coater. SEM images were taken using an extra high-resolution scanning electron microscope, Magellan TM400L, operating at 2 kV.

Focused Ion Beam and Scanning Electron Microscopy (FIB-SEM)

Cross-section measurements of the samples were conducted using a DualBeam Focused Ion Beam (FIB-SEM) system (Helios NanoLab 460F1, FEI, USA).

Fourier Transform Infrared Spectroscopy (FTIR)

Peptide stock solution was diluted to a final concentration of 1 mg/mL in deuterated media (Tris buffer in D_2O or 1 M DCl). Then, each peptide solution was deposited on a CaF2 plate and dried under vacuum. Infrared spectra were recorded using a Nicolet 6700 FTIR spectrometer with a deuterated triglycine sulfate (DTGS) detector (Thermo Fisher Scientific, MA, USA). The measurements were taken using 4 cm^{-1} resolution and an average of 2000 scans. The absorbance maximal values were determined by the OMNIC analysis program (Nicolet). Each spectrum was deconvoluted.

Contact Angle measurements

Contact angle measurements were carried out using a Theta Lite optical tensiometer (Attension, Finland).

NMR Structural Analysis

Samples were prepared by dissolving peptide in d_6-ethanol (100 mg/mL). Five microliters of this solution were transferred to 450 µL of each of the three different aqueous solutions (10 mM HCl, pH=1; 10 mM NaCl, pH=7; 10 mM d_{11}-tris buffer, pH=8.5), each containing 10% (v/v) D_2O, to obtain a final concentration of 1 mg/mL.

NMR experiments were performed on a Bruker AVII 500 MHz spectrometer operating at the proton frequency of 500.13 MHz, using a 5-mm selective probe equipped with a self-shielded xyz-gradient coil at 27.2 °C. The transmitter frequency was set on the water signal and calibrated at 4.811 ppm. Correlation spectroscopy (COSY),[2] total correlation spectroscopy (TOCSY)[3] using the MLEV-17 pulse scheme for the spin lock (150 ms),[3] and Rotating frame Overhauser Effect spectroscopy (ROESY) experiments using an optimized mixing time of 200 ms[3-5] were acquired using gradients for water saturation under identical conditions.[6]

Spectra were processed and analyzed with TopSpin (Bruker Analytische Messtechnik GmbH) and SPARKY3 software.[7] Resonance assignment followed the sequential assignment methodology developed by Wüthrich.[8]

The three-dimensional structures of the peptide were calculated using XPLOR (version 3.856)[9] by hybrid distance geometry-dynamical simulated annealing. Peak intensities were manually assigned as strong (2.5 Å), medium (3.5 Å), weak (4.5 Å) and very weak (5.5 Å) with a ±0.5 Å error. Parameters were introduced using charges derived from the electrostatic potential charges of single amino acids calculated at the UHF/6-31þG(d,p) and the Amber forcefields.[10] Fifty initial structures were generated. The ROE energy was introduced as a square-well potential. Molmol[11] was used to create the final ensemble of structures. Low energy structures chosen for further

analysis had no ROE violations, deviations from ideal bond lengths of less than 0.05 Å, and bond angle deviations from ideality of less than 5º. Hydrogen bonds were determined using constraints relaxed by 0.4 Å and 20°, and figures were produced using Chimera from the University of California, San Francisco (supported by NIH P41 RR-01081).[12]

Electrostatic free energies were derived from finite difference solutions of the Poisson-Boltzman equation using the DelPhi program.[13] Electrostatic potential charges calculated at the UHF/6-31þG(d,p) were employed and a full Coulombic calculation was performed. The positive and negative 0.1 *k*T/*e* isopotential surfaces were presented using Chimera.[12]

Molecular Dynamics

All simulations were performed using the NAMD 2.11 program.[14] Each system was subjected to 3000 steps of energy minimization (Newton–Raphson method) before any MD trajectory was run in order to relax conformational and structural tension. Both temperature and pressure were controlled by two different strategies depending on the sub-cycle by which it was run. Due to fast convergence, the weak coupling method (Berendsen thermobarostat[15]) was used to heat the system and rapidly equilibrate its pressure and temperature around 1 bar and 298 K, respectively. The relaxation times used for the coupling were 1 and 10 ps for temperature and pressure, respectively. For final equilibration and for all production runs, both temperature and pressure were controlled by the Nose–Hoover piston[16] combined with the piston fluctuation control of temperature implemented for Langevin dynamics.[17] Pressure was kept at 1.01325 bars, the oscillation period was set to 1 ps while the piston decay time was set to 0.001 ps. The piston temperature was set to the same value as the thermostat control, 298 K, which used a damping

coefficient of 2 ps. The integration step was 2 fs in all simulations. The temperature, density and pressure of each examined model were equilibrated by three consecutive MD runs. First, an NVT-MD simulation at 298 K was run for 1 ns using the Berendsen thermostat, the resulting atom velocities and coordinates being used as the starting point for a 1 ns NPT-MD run using the same procedure (298 K, 1 bar pressure). The end of this simulation was the starting point of the final 1 ns NPTMD simulation (298 K, 1 bar pressure) using the combination of Langevin dynamics with the Nose–Hoover piston oscillator, ensuring their ultimate equilibration through a correct thermodynamic ensemble. The last step of any last equilibration run was the starting point of the productive trajectories presented in this work (298 K, 1 bar pressure). The coordinates of all the production runs were saved every 2 ps for further analysis.

Simulated Annealing Molecular Dynamics (SA-MD)

Prior to the production cycles with the modified SA-MD, the system was equilibrated. 0.5 ns of NVT-MD at 500 K were used to homogeneously distribute the solvent and ions in the box. Next, thermal equilibration was performed for 0.5 ns in the constant-NVT ensemble at 298 K, followed by density relaxation for 0.5 ns in the constant-NPT ensemble at 298 K. The last snapshot of the NPT-MD was used as the starting point for the conformational search process. This initial structure was quickly heated to 900 K at a rate of 50 K ps 1 to force the molecule to jump to a different region in conformational space. Along 10 ns, the 900 K structure was slowly cooled to 500 K at a rate of 1 K per second. A total of 500 structures were selected and subsequently minimized during the first cycle of modified SA-MD. The resulting minimum energy conformations were stored in a rank-ordered library of low energy structures. The lowest energy

structure generated in a modified SA-MD cycle was used as the starting conformation of the next cycle. Both energy computation and simulation conditions were set using the same structure shown in plain MD. Atom pair distance cut-offs were applied at 14.0 Å to compute the van der Waals and the real space terms of the electrostatic interactions within the framework of Ewald summations. The reciprocal space was computed by interpolation of the effective charge into a charge mesh with a grid thickness of 1 point per $Å^3$. [18] In order to avoid discontinuities in the potential energy function, non-bonding energy terms were forced to slowly converge to zero, by applying a smoothing factor from a distance of 12.0 Å. Both temperature and pressure were controlled using the combination of Langevin dynamics with the Nose–Hoover piston oscillator,[16,17] ensuring their ultimate equilibration through a correct thermodynamic ensemble with a numerical integration step of 2 fs. All MD simulations were performed using the NAMD 2.11 program.[14]

Identification of weak interactions was based on the following geometric criteria: (a) for X–H···Y hydrogen bonds (X, being nitrogen or oxygen, Y being oxygen or fluorine) the distance between the hydrogen and acceptor Y atom is shorter than 3.0 Å; (b) for π-π stacking, the distance between the center of mass of the stacked rings is shorter than 5.5 Å; (c) for N–H···π interactions, the distance between the hydrogen and the center of mass of the ring is shorter than 3.0 Å.

Preparation of Doxorubicin-loaded Spheres

Doxorubicin-loaded spheres were prepared by diluting a peptide stock solution (100 mg/mL) to a concentration of 1 mg/mL in aqueous medium (either Tris buffer or HCl) containing doxorubicin at a concentration of 0.05 mg/mL.

Fluorescence Microscopy

A 30 µL drop containing the doxorubicin-loaded sphere solution was drop-casted on a glass cover slip and allowed to dry at RT. A 30 µL drop of doxorubicin in aqueous medium (HCl or tris buffer) was also drop-casted on a glass cover slip as a control.

Images were taken using a fluorescence microscope (Carl Zeiss, Axio Vision). Samples were excited at 510 nm.

Drug Release Study

Doxorubicin-loaded spheres were prepared as described. After the self-assembly process, samples were left to precipitate overnight, the aqueous medium was decanted, and the peptide assemblies were re-dispersed in PBS (10 mM NaCl, pH=7.4, 150 mM). Then, 2 mL of the doxorubicin-loaded peptide were transferred into a dialysis bag (MWCO 3 kDa), and the bag was immersed in 45 mL of PBS at RT. One mL of the buffer outside the dialysis bag was taken at different time intervals for 9 days, for fluorescence measurements. The volume of the solution was kept constant by adding 1 mL of the original PBS solution after each sampling. The fluorescence measurements were performed at RT using a fluorescence spectrometer (Edinburgh instruments FLS920). The emission spectra were collected from 500 nm to 750 nm, with an excitation wavelength of 480 nm.

Protein Adsorption

A 50 µL drop of BSA solution (150 µM in PBS) was applied onto the substrate in a Petri dish. The plate was placed in a humidified incubator at 37 °C for 2 hours. The substrates were then rinsed 3 times with PBS (pH=7.43, 10 mM NaCl, 150 mM), and transferred into test tubes with 1 mL of 2% (w/w) SDS. The samples were shaken for 60 min and sonicated for 20 min at RT to detach the adsorbed proteins. Protein concentrations in the SDS solution were determined using the Non-interfering protein assay (Calbiochem, USA) according to the manufacturer's instructions, using a microplate reader (Synergy 2, BioTek) at 480 nm. All measurements were performed in triplicate and averaged.

Preparation of GOx-loaded Spheres

GOx-loaded spheres were prepared by diluting a peptide stock solution (100 mg/mL) to a concentration of 1 mg/mL in Tris buffer containing GOx at a concentration of 100 µg/mL.

Preparation of Surfaces Coated with GOx-loaded Spheres

A drop of 150 µL of solution containing GOx-loaded spheres was drop-casted on 1×1 cm^2 glass substrates. Then the samples were left to dry, dipped in TDW to remove excess enzyme and peptide, and dried again.

Hydrogen Peroxide Release from Spheres

GOx loaded spheres were prepared as described above. After the self-assembly process, samples were left to precipitate overnight, the aqueous medium was decanted, and the peptide assemblies were re-dispersed in PBS (10 mM NaCl, pH=7.4, 150 mM). Then, 2 mL of the GOx-loaded peptide were transferred into a dialysis bag (MWCO 3 kDa), and the bag was immersed in 45 mL of PBS at RT. 100 µL of the buffer outside the dialysis bag was taken out at different time intervals to react with HRP/$ABTS^{2-}$ solution. After 10 minutes, a 1% SDS solution was added to stop the reaction. $ABTS^{\bullet-}$ concentration was determined using a microplate reader (Synergy 2, BioTek) at 414 nm. Hydrogen peroxide concentrations were calculated from the molar ratios.

Preparation of fluorescent labeled GOx

10 mg of GOx were dissolved in 5 mL of HEPES buffer (0.1 M, pH=8.1). Then, 50 µL of Atto590-NHS in dry DMF (2 mg/mL) were added to the solution and left to stir for 1 hr at RT. The resulting mixture was separated on a PD-10 column, using HEPES as the eluent. The number of fluorophores on each protein was determined using a spectrophotometer (Shimadzu) at 595 nm.

Quantification of GOx on the spiky spheres

Labelled GOx was dissolved in Tris buffer (10 mM, pH=8.5) and the fluorescence of the solution was measured. After the self-assembly process, the peptide was left to precipitate and the

supernatant fluorescence was measured. The concentration of protein in solution and on the spheres was calculated by plotting a concentration calibration chart.

Bacterial Growth

E.coli (ATCC 25922) were grown in tryptic soy broth (TSB) medium at 37 ˚C, for 6 hr, in loosely capped tubes with agitation (120 rpm), to late logarithmic phase. Then, the bacteria were centrifuged and washed 3 times with PBS, re-suspended, and diluted to 105 CFU/mL with either TSB or 2% (w/v) glucose in TSB.

Antibiotic Release

Gentamicin-loaded spheres were prepared by diluting the peptide stock solution (100 mg/mL) to a concentration of 1 mg/mL in aqueous medium (either Tris buffer or HCl) containing gentamicin at a concentration of 0.5 mg/mL. Then, a 100 µL drop of the solution containing gentamicin-loaded spheres was drop-casted on 1×1 cm^2 glass substrates and the samples were left to dry. In order to remove excess drug and peptide, the substrates were dipped in TDW and dried again. Subsequently, the substrates were placed in 3 mL of PBS (10 mM, pH=7.4) and incubated for 24 hr. After incubation, 10 µL were collected from the PBS and placed on an agar plate streaked with *E.coli*. The plates were incubated at 37 ˚C overnight. After incubation, the zone of the inhibition diameters were measured and compared.

Antifouling property of the Peptide Assemblies

Three mL of the bacterial culture were transferred to each petri dish, the glass slides were placed horizontally in the plate and incubated in a humidified incubator at 37 ˚C for either 24 hr or 3 days. One additional mL of TSB was added to each plate after two days to ensure a sufficient supply of nutrients.

After incubation, the substrates were gently rinsed with 3 mL of PBS and transferred into test tubes with 5 mL of PBS. Then, the test tubes were sonicated for 1 min to detach bacteria from the substrates, and vortexed for 15 seconds. The number of viable bacteria was determined by plating the samples in 10-fold serial dilutions on Lysogeny broth (LB) agar plates.

Antibacterial Dual Activity of the Surfaces

A drop of 150 µL of the bacterial culture was gently placed on each substrate, and the substrates were placed horizontally in the plate and incubated in a humidified incubator at 37 ˚C for 1 hr. After incubation, the substrates were gently rinsed with 1 mL of PBS, and transferred into test tubes with 3 mL of PBS. Then, the test tubes were sonicated for 1 min to detach bacteria from the substrates, and vortexed for 15 s. The number of viable bacteria was determined by plating the samples in 10-fold serial dilutions on LB agar plates.

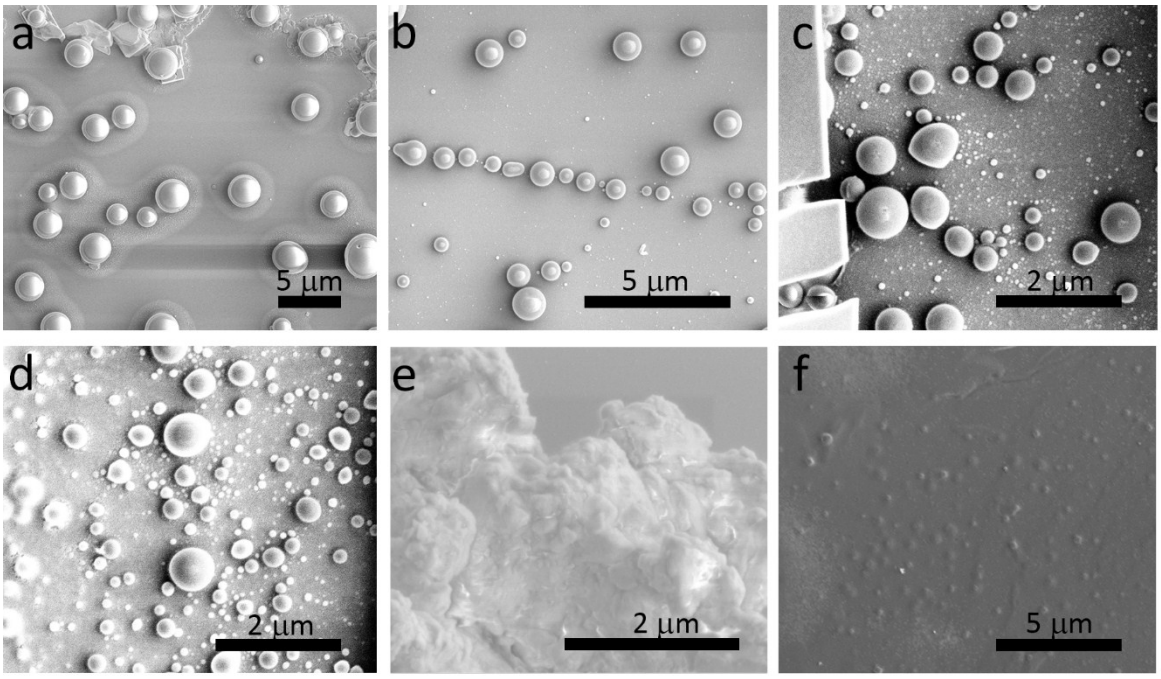

Figure S1. Self-assembly of the peptide at different pH values in HCl : (a) pH=1, (b) pH=2, (c) pH=3, (d) pH=4, (e) pH=5 and (f) pH=6. The average diameter of the spheres formed in acidic medium decreases with increasing pH until they are not predominant in the sample.

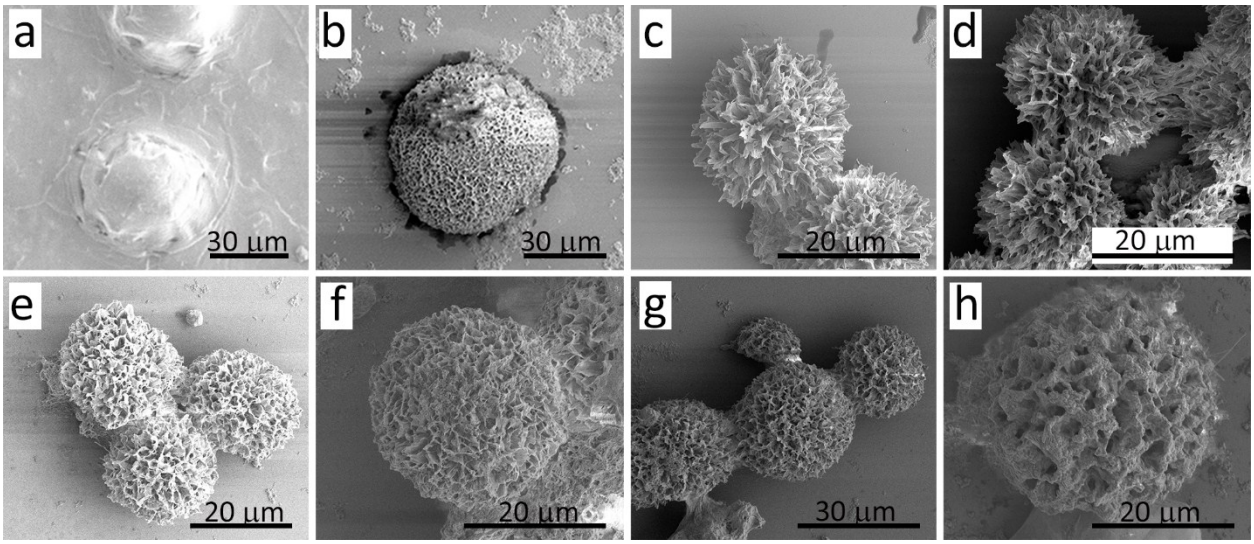

Figure S2. Self-assembly of the peptide at different pH values in tris buffer (10 mM): (a) pH=6.5, (b) pH=7, (c) pH=7.5, (d) pH=8, (e) pH=9, (f) pH=9.5, (g) pH=10 and (h) pH=10.5.At a neutral pH the surface is mostly covered with undefined aggregates. When the pH is increased, the spiky spheres are formed. The higher the pH the denser each sphere becomes.

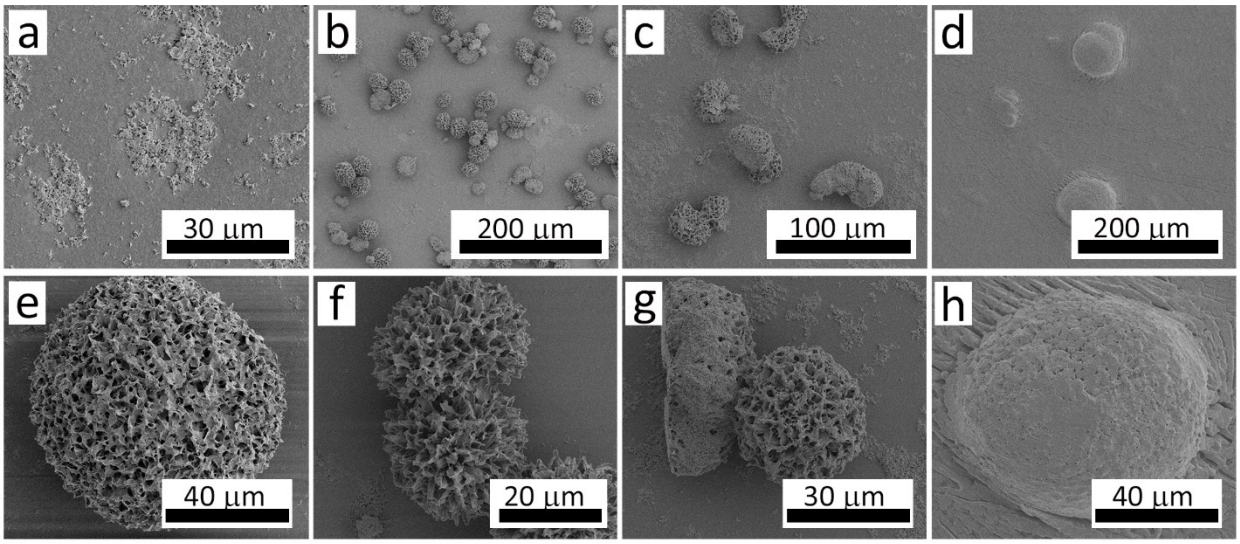

Figure S3. Self-assembly of the peptide in different concentrations of TRIS. The upper panel shows the coverage of the surface by the peptide structures and the lower panel shows the morphology of the structures: (a) and (e) 1 mM, (b) and (f) 5 mM, (c) and (g) 15 mM and (d) and (h) 20 mM.

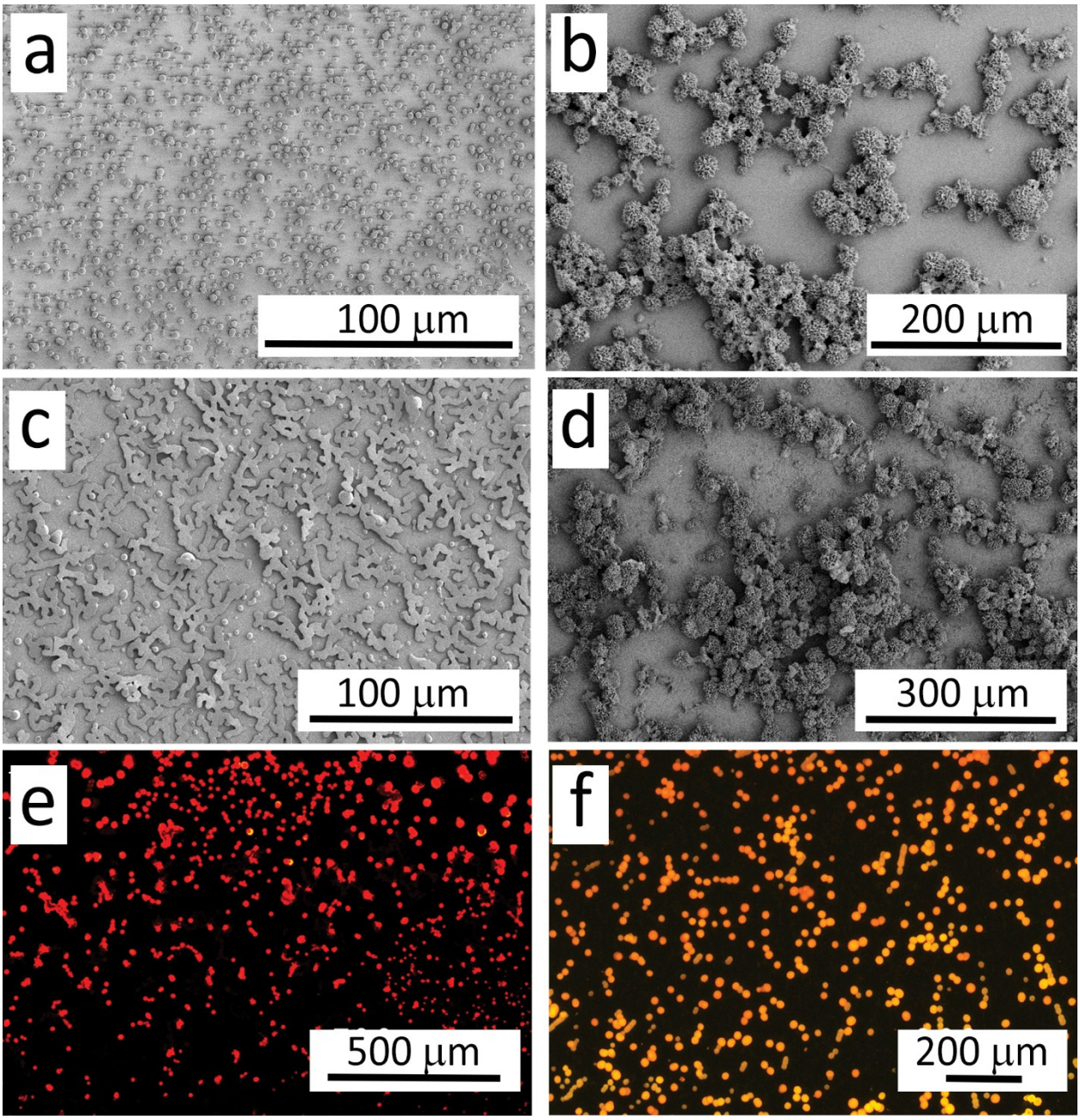

Figure S4. (a-b) The SEM micrographs demonstrate the extent of coverage of the substrates by (a) smooth spheres, (b) spiky spheres. (c-d) Improvement of the coverage by applying a few drops of solution containing (c) smooth spheres, (d) spiky spheres. (e-f) Fluorescent microscopy micrographs, which demonstrate the extent of coverage of the substrates by (e), smooth spheres with doxorubicin and (f) spiky spheres with doxorubicin.

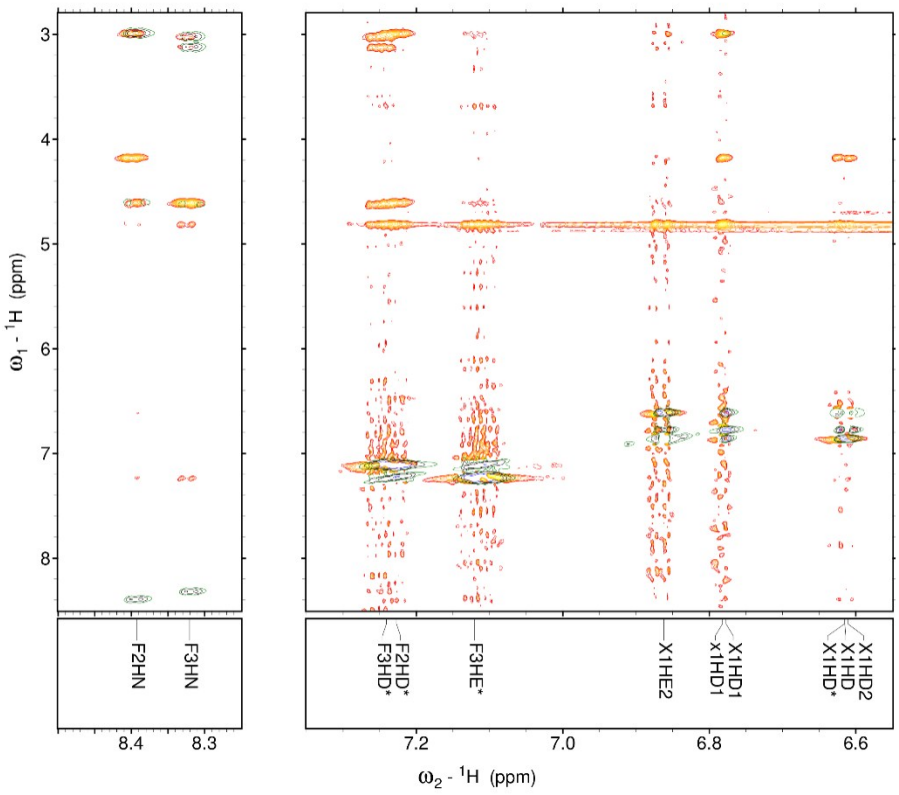

Figure S5. TOCSY NMR (green-blue) overlaid on ROESY (red-yellow) spectrum from acidic conditions.

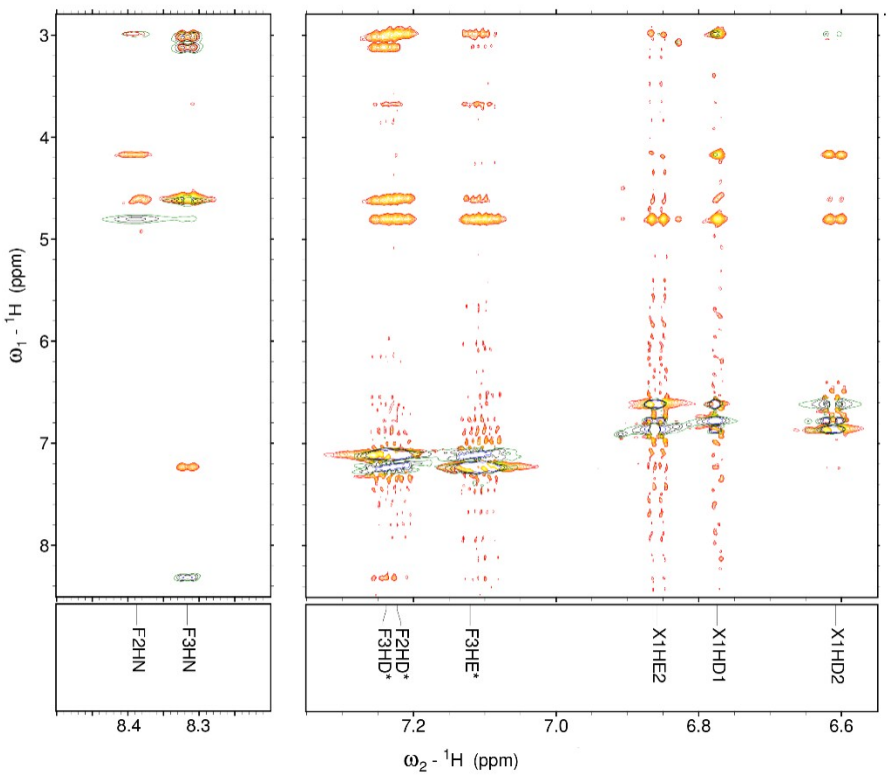

Figure S6. TOCSY NMR (green-blue) overlaid on ROESY (red-yellow) spectrum from salt conditions.

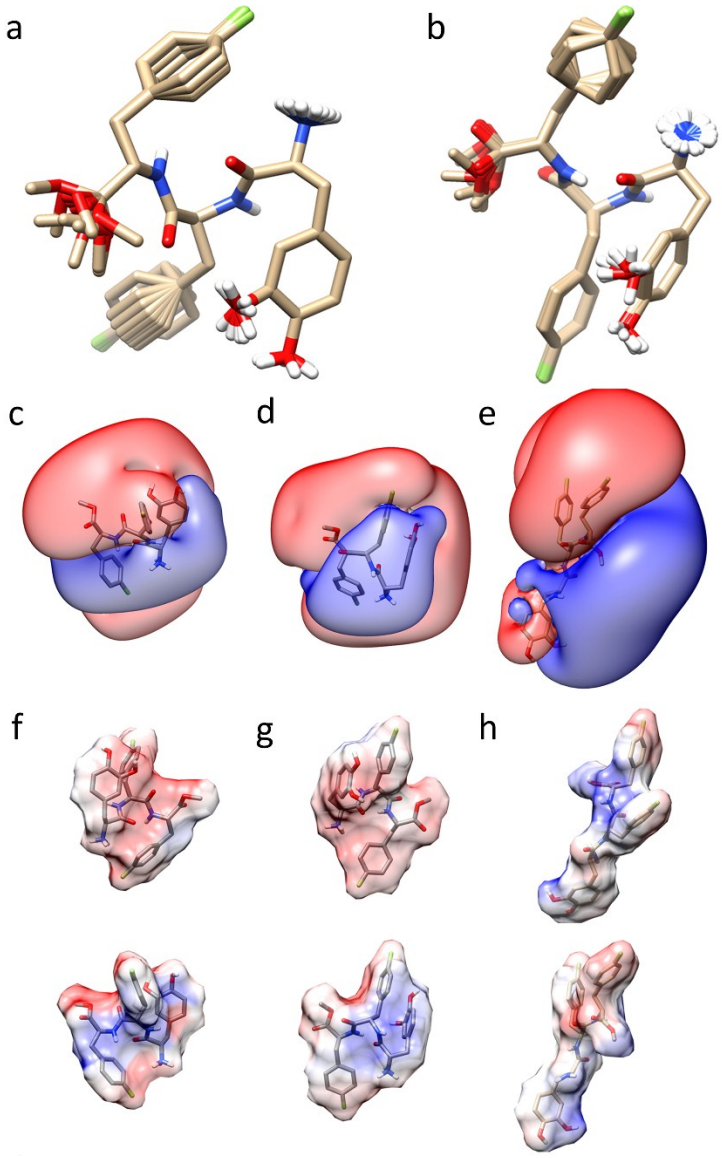

Figure S7. Structural Analysis and self-assembly mechanism by NMR. NMR-derived ensembles under (a) acidic and (b) salt conditions; Electrostatic isosurfaces for ± 0.1 kT/e (red is negative, blue is positive) (c) acidic, (d) salt and (e) basic conditions representative structures; Van der Waals surfaces colored by electrostatic potential from two views (red is negative, blue is positive – the intensity is proportional to the strength of the potential) for (f) acidic, (g) salt and (h) basic conditions.

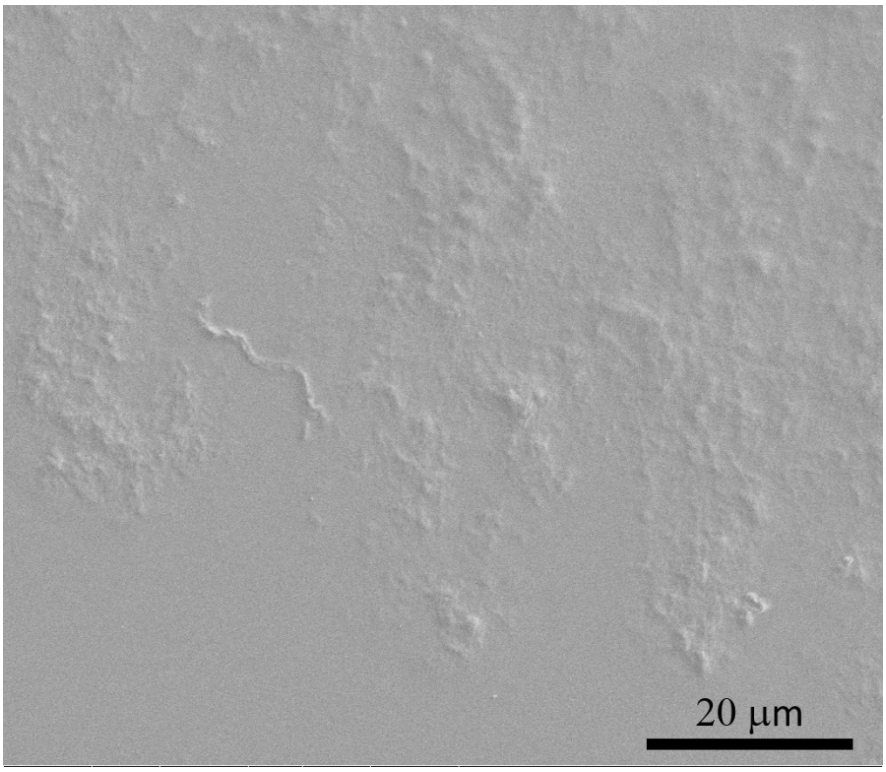

Figure S8. SEM image of peptide under salt conditions exhibiting no supramolecular structures.

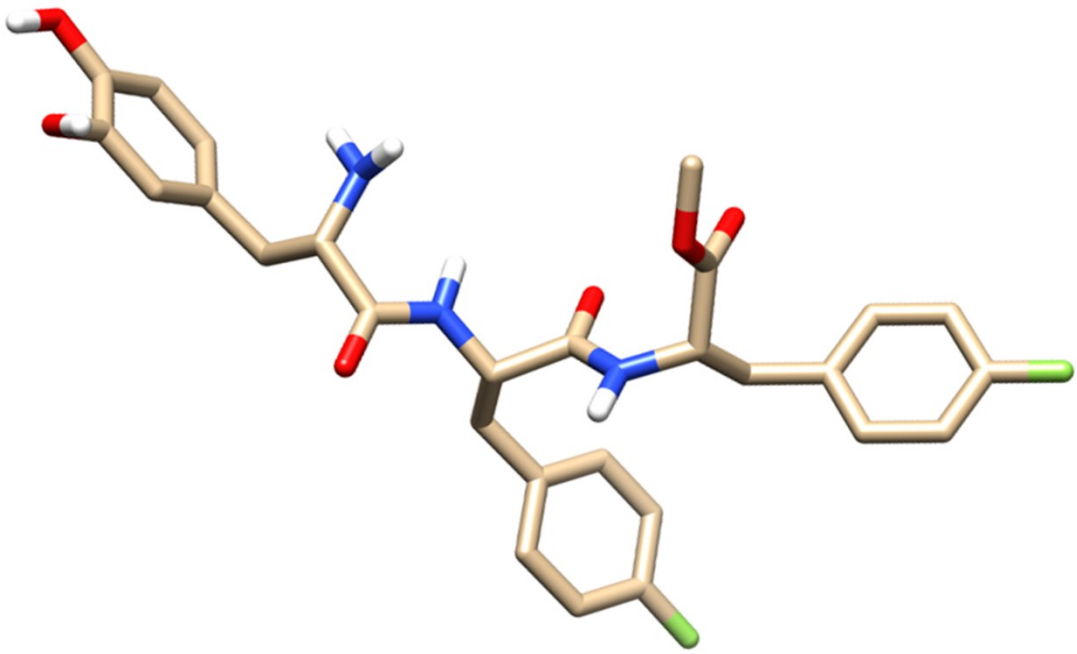

Figure S9. MD-derived structure of the basic monomer.

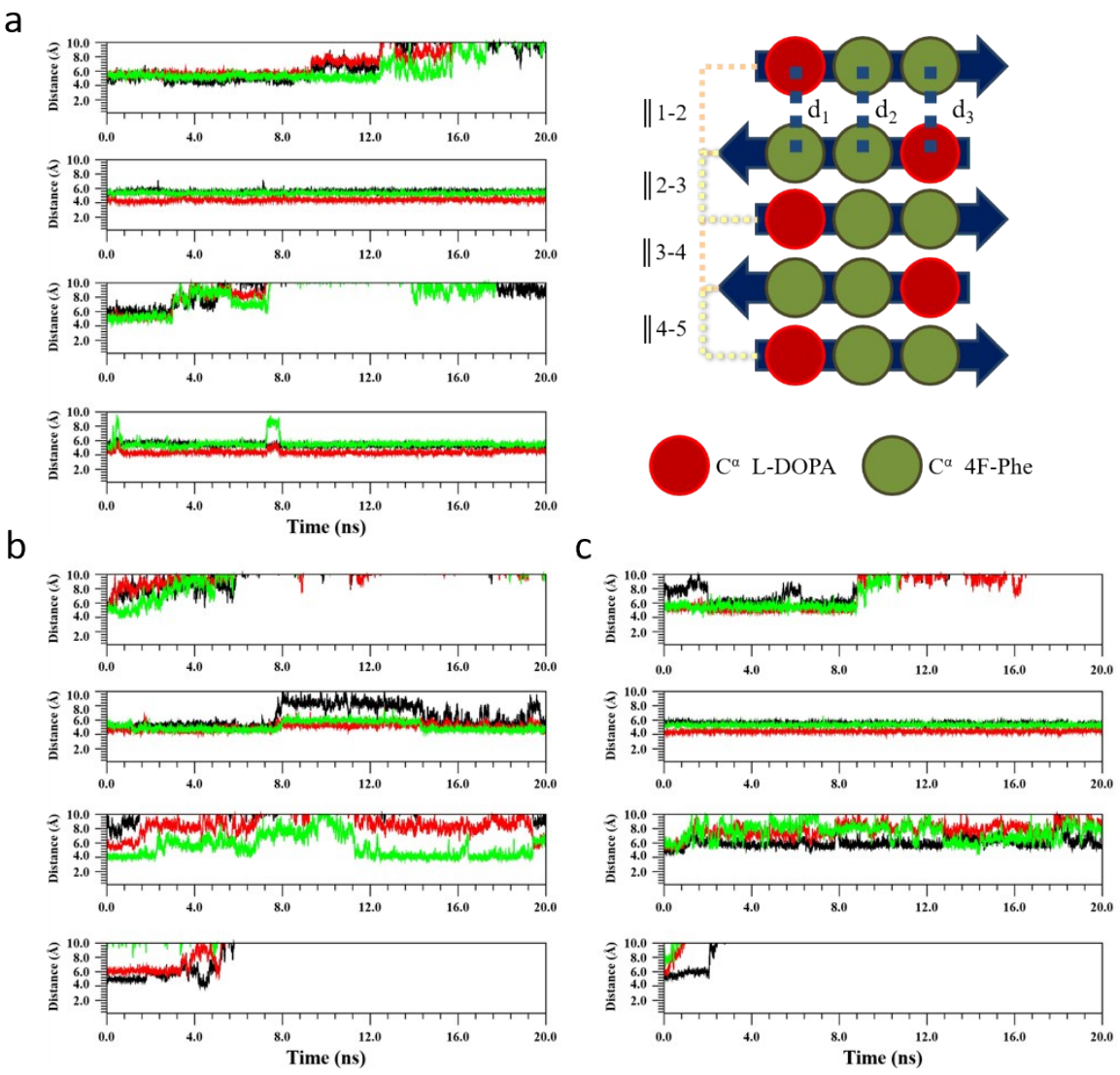

Figure S10. Time evolution of Cα-Cα distances. Each plot shows the distances between chains during the simulations under (a) acidic, (b) salt and (c) basic conditions. Black line represents d_1, red is d_2 and green is d_3.

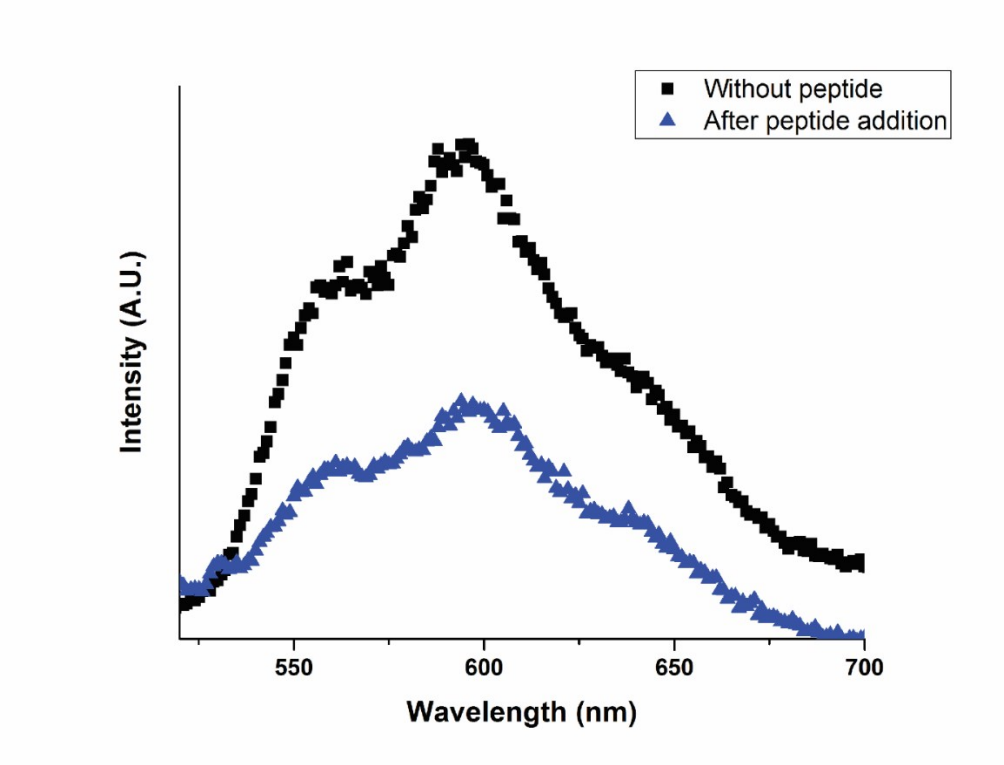

Figure S11. The reduction in the fluorescence intensity of doxorubicin upon the self-assembly of the peptide.

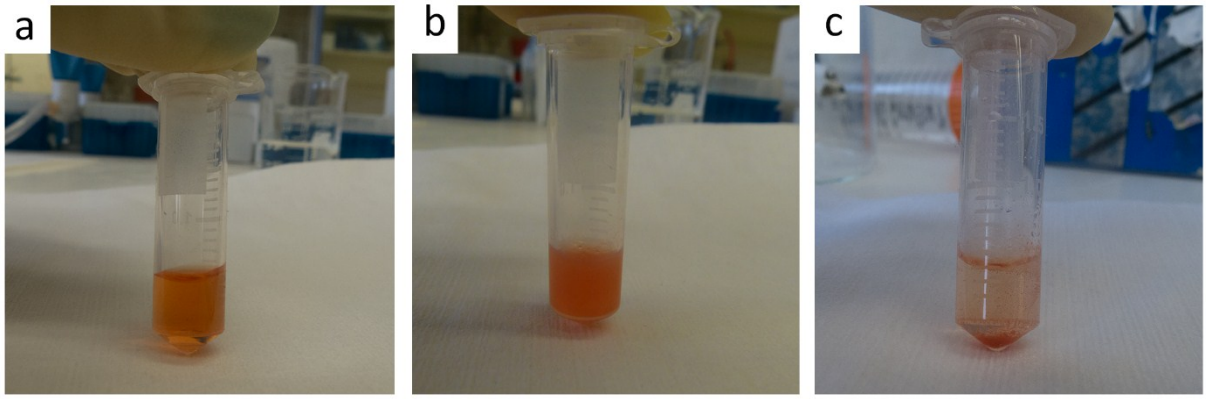

Figure S12. Doxorubicin encapsulation/adsorption. (A) Doxorubicin in TRIS buffer, (B) the solution becomes opaque with peptide addition, and (C) stained peptide assemblies precipitate during night, leaving a clear solution.

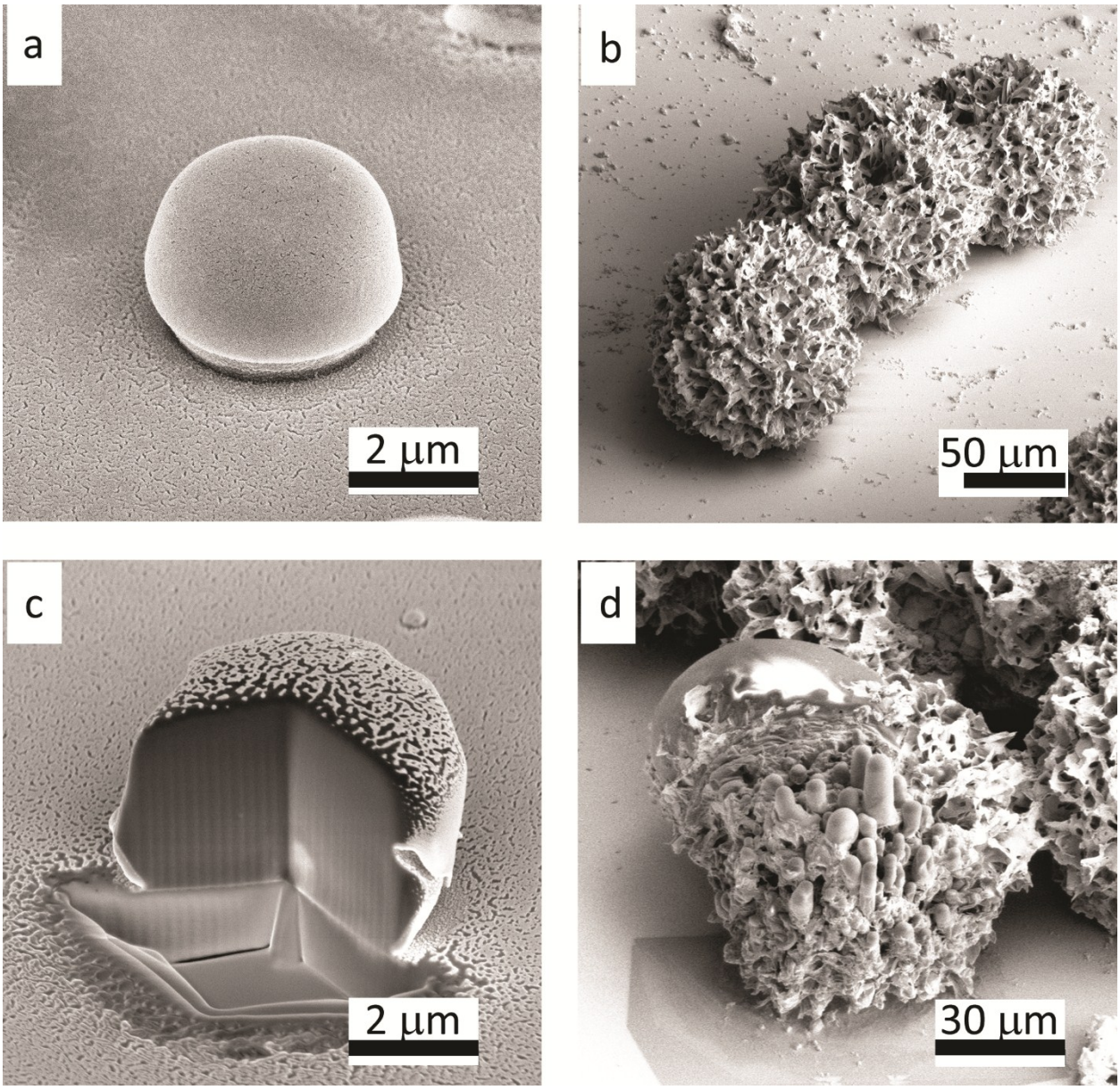

Figure S13. Scanning electron micrographs of peptide assemblies before (upper panel) and after (lower panel) FIB-SEM. (a) and (c) smooth spheres, (b) and (d) spiky spheres.

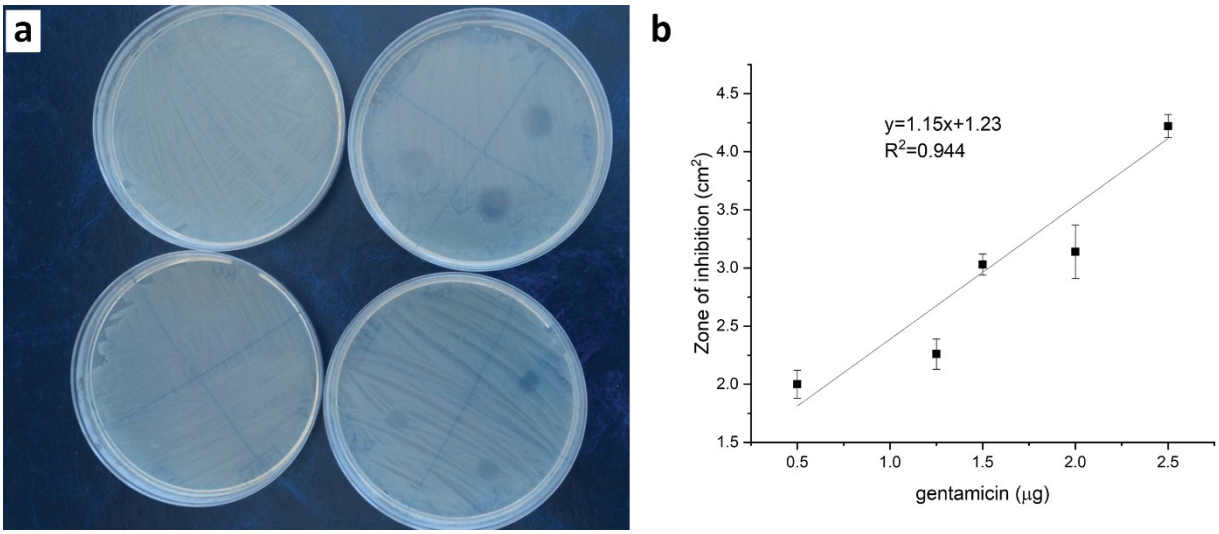

Figure S14. Gentamicin release from the peptide assemblies after overnight incubation. (a) On the left, agar plates on which buffer incubated with bare surfaces was applied. On the upper right, zones of inhibition formed after applying buffer that was incubated with surfaces modified with spiky spheres. On the lower right, zones of inhibition formed after applying buffer that was incubated with surfaces modified with smooth spheres. (b) Gentamicin calibration table.

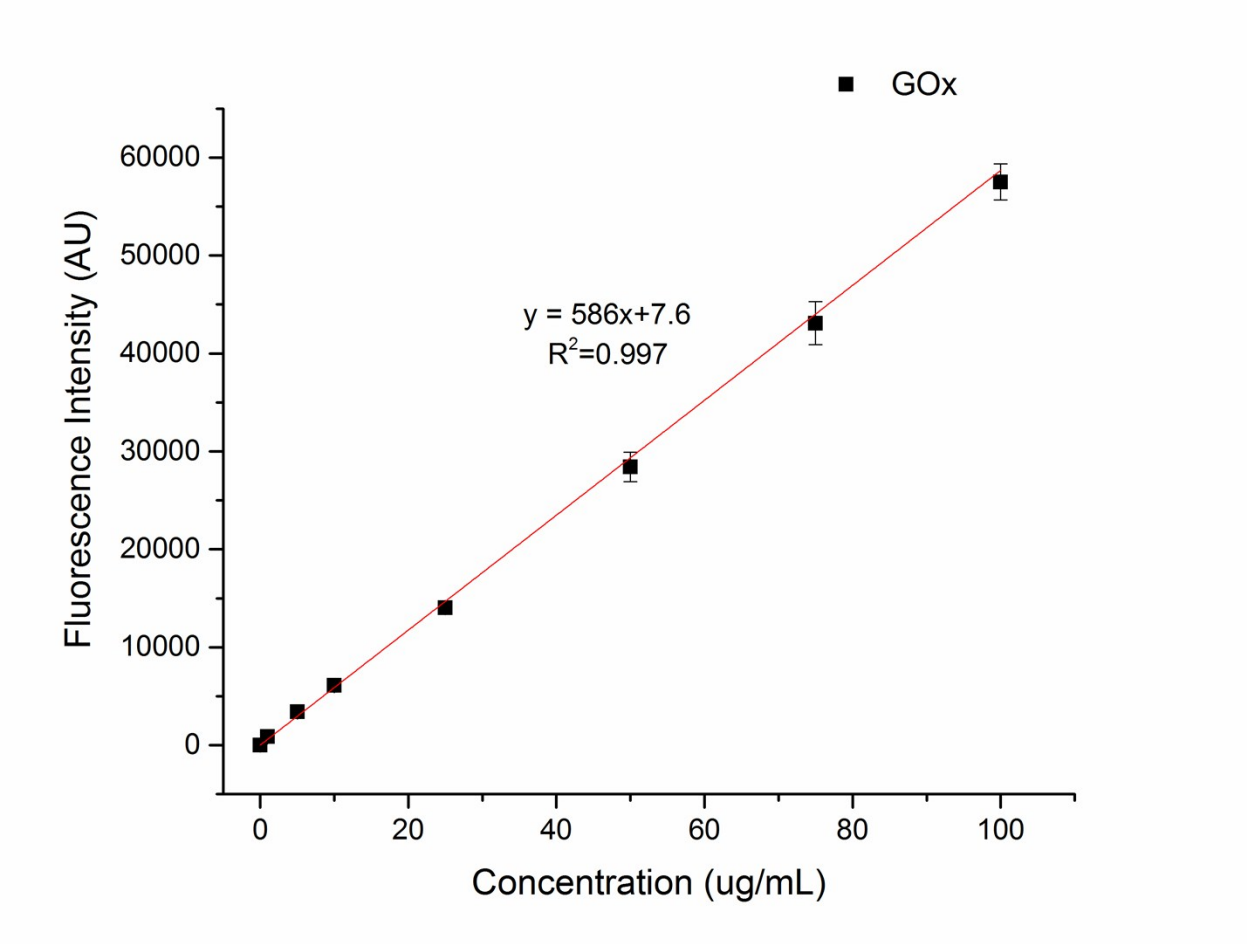

Figure S15. Calibration chart of GOx concentration. The graph plots the concentration of GOx solution *vs.* the fluorescence intensity of the $Atto_{590}$ fluorescent label. The ratio of GOx to $Atto_{590}$ was calculated to be 1:1.

GOx amount on spheres: $$y = 586x + 7.6 \rightarrow x = \frac{y - 7.6}{586} => 64\ \mu g$$

GOx lot result: 248,073 U/gr

Enzymatic units on spheres: $$248{,}073\ \frac{U}{gr} \times 64 \cdot 10^{-6}\ gr = 15.8\ U \cong 16\ U$$

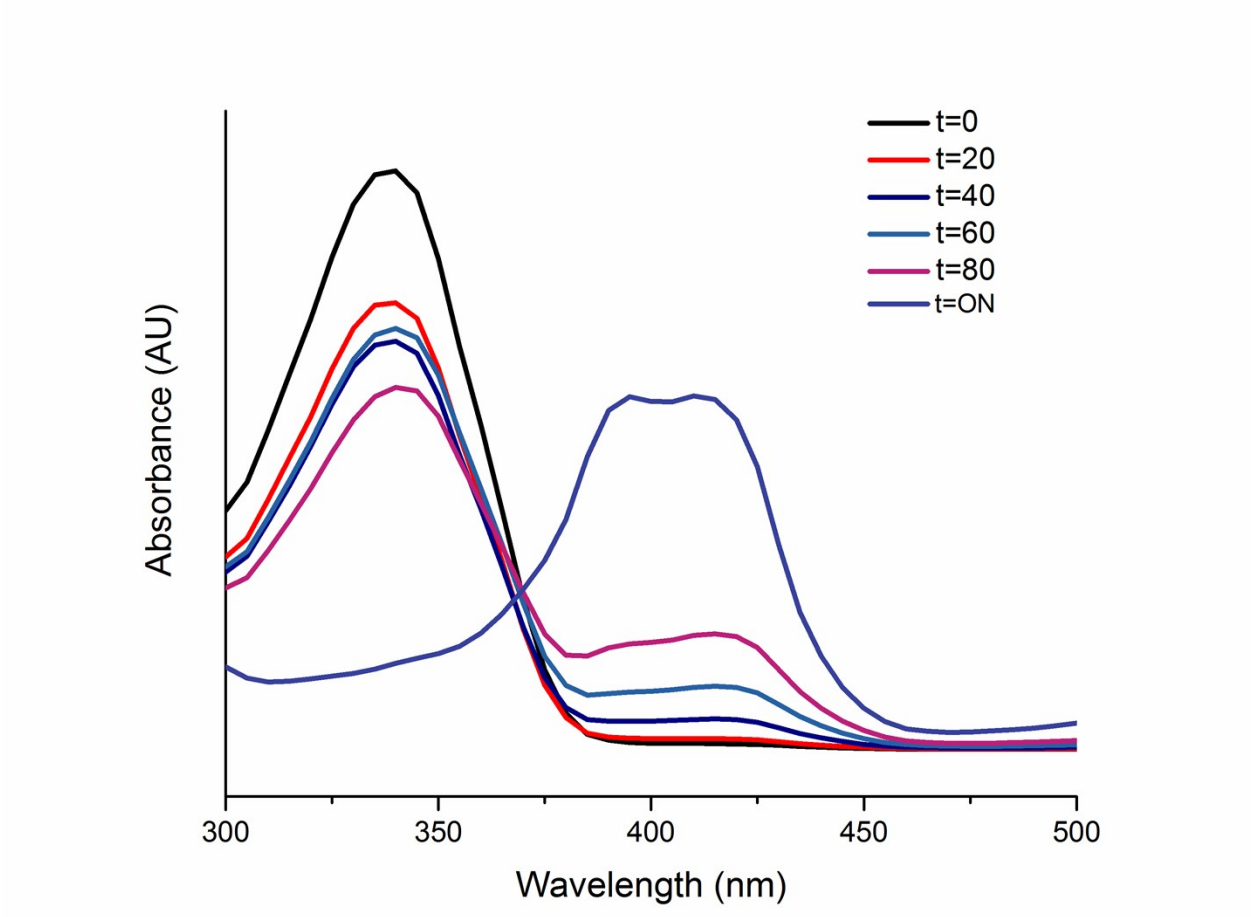

Figure S16. Absorption changes upon oxidation of $ABTS^{2-}$. The plot presents the decrease in absorption at λ = 340 nm, and the increase in absorption at λ = 414 nm. After an overnight incubation, only absorption at λ = 414 nm was detected.

Residue	HN	Hα	Hβ	Others
DOPA1		4.17		Hδ1 6.78; Hδ2 6.61; Hε2 6.86
4f-Phe2	8.40	4.60	2.99, 2.99	Hδ 7.23
4f-Phe3	8.32	4.61	3.02, 3.12	Hδ 7.24
-OMe				CH_3 3.67

Table S1. ^{1}H-NMR Table of assignments - Acidic (ppm).

Residue	HN	Hα	Hβ	Others
DOPA1		4.17		Hδ1 6.60; Hδ2 6.77; Hε2 6.85
4f-Phe2	8.38	4.61	2.98, 2.98	Hδ 7.22
4f-Phe3	8.31	4.60	3.00, 3.11	Hδ 7.23; Hε 7.12
-OMe				CH_3 3.67

	Acidic	**NaCl**
NOE Connectivity		
Total	21	24
i,i	14	15
i,i+1	7	8
i,i+2	-	1
RMSD		
Non-violated	49/50	43/50

Table S2. ^{1}H-NMR Table of assignments – Salt (ppm).

backbone	0.175	0.04
heavy	0.888	0.694
Low-energy ensembles (10 members each)		
backbone	0.004	0.001
heavy	0.616	0.608

Table S3. Ensemble statistics.

Single chain simulations (SA-MD)		
	I-II	**III**
Na^+	0	0
Cl^-	1	1
H_2O	8439	8439
a b c (Å)	46x46x46	46×46×46

Assembly models (MD)			
	1	**2**	**3**
# chains	5	5	5
Na^+	0	0	0
Cl^-	178	5	0
H_3^+O	173	0	0
H_2O	8439	8439	8439
a b c (Å)	66×66×66	66×66×66	66×66×66

Table S4. Chemical constitution of all studied systems. I-III represent different ionization states of the single molecule, whereas sequences (I-II) stand for $–NH_3^+$ terminated peptide and (III) stands for $–NH_2$ terminated peptide. Sequences 1-3 represent clusters of the peptides under different pH conditions (different ionization), whereas (1) stands for acidic pH, (2) stands for neutral pH and (3) stands for basic pH (pH=9).

Condition	pair	d_1	d_2	d_3
Acidic	1-2	7.3±2.4	11.1±3.3	9.3±2.4
	2-3	5.3±0.1	4.4±0.2	5.3±0.1
	3-4	9.3±2.4	11.1±3.3	9.3±2.4
	4-5	5.6±0.6	4.4±0.3	5.6±0.6
Salt	1-2	7.5±1.2	7.8±1.0	7.5±1.2
	2-3	5.3±0.1	4.4±0.2	5.3±0.1
	3-4	6.2±0.9	6.1±0.6	6.4±0.4
	4-5	29.0±9.8	29.0±10.3	29.0±9.7
Basic	1-2	11.9±3.1	11.0±2.0	12.03.7
	2-3	5.5±1.4	5.0±0.5	5.1±0.6
	3-4	12.4±2.0	6.0±2.7	5.5±1.6
	4-5	21.2±11.8	21.9±11.5	22.4±10.3

Table S5. Averaged inter-strand distances at the end of the simulation. All distances are expressed in Å. Each magnitude corresponds to the distance between pairs of alpha carbons that belong to strands that were adjacent within the initial β-sheet assembly.

1 S. Maity, S. Nir, T. Zada and M. Reches. *Chem.Commun.* 2014, ***50***, 11154.
2 W. P. Aue, E. Bartholdi and R. R. Ernst, *J. Chem. Phys.* 1976, ***64***, 2229.
3 A. Bax, and D. G. Davis. *J. Magn. Reson.* 1985, ***65***, 355.
4 M. Piotto, V. Saudek and V. Sklenar. *J. Biomol. NMR* 1992, ***2***, 661.
5 V. Sklenar, M. Piotto, R. Leppik and V. Saudek, *J.Magn.Reson.Ser.A* 1993, ***102***.
6 M. L. Liu, Xi-a. Mao, C. Ye, H. Huang, J.K. Nicholson and J. C. Lindon. *J. Magn. Reson.* 1998*,* ***132***, 125.
7 T. D. Goddard and D. G. Kneller, SPARKY 3, University of California, San Francisco.
8 K. Wüthrich, In *NMR of Proteins and Nucleic Acids*, John Wiley & Sons, New York, 1986.
9 M. Nilges, J. Kuszewski and A.T. Brunger, In *Computational aspects of the study of biological macromolecules by nuclear magnetic resonance spectroscopy*; J.C. Hoch, F.M. Poulsen, C. Redfield, eds.; Plenum Press: New York, 1991.
10 D. A. Pearlman, D. A. Case, J. W. Caldwell, W.S. Ross, C. E. Cheatman III, S. Debolt, D. Ferguson, G. Siebel and P. Kollman. *Comput. Phys. Commun.* 1995, ***91***, 1.
11 R. Koradi, M. Billeter and K. Wuthrich. *J. Mol. Graph.* 1996, ***14***, 51.
12 E. F. Pettersen, T. G. Goddard, C. C. Huang, G. S. Gouch, D. M. Greenblatt, E.C. Meng and T. e. Ferrin. *J. Comput. Chem.* 2004, ***25***, 1605.
13 B. Honig, K. Sharp and A. S. Yang. *J. Phys. Chem.* 1993, ***97***, 1101.
14 J. C. Phillips, R. Braun, W. Wang, J. Gumbart, E. Tajkhorshid, E. Villa, C. Chipot, R.D.Skeel, L. Kale and K. Schulten. *J. Comput. Chem*. 2005, ***26***, 1781.
15 H. J. C. Berendsen, J. P. M. Postma, W. F. Vangunsteren, A. Dinola and J. R. Haak. *J. Chem. Phys*. 1984, ***81***, 3684.
16 G. J. Martyna, D. J. Tobias and M. L. Klein. *J. Chem. Phys*. 1994, ***101***, 4177.
17 S. E. Feller, Y. H. Zhang., R. W. Pastor and B. R. Brooks. *J. Chem. Phys.* 1995, ***103,*** 4613.
18 A. Toukmaji, C. Sagui, J. Board and T. Darden. *J. Chem. Phys.* 2000, ***113,*** 10913.